SINERGI Vol. 30, No. 3, October 2026: 927-942
http://publikasi.mercubuana.ac.id/index.php/sinergi
http://doi.org/10.22441/sinergi.2026.3.019

Evaluation of initialization strategies in fuzzy self-tuning PI control for a 4×4 methanol–water distillation system

Abdul Wahid[1]*, Fathur Rahman[1], Dianursanti Dianursanti[2]
[1]Process Systems Engineering Lab., Department of Chemical Engineering, Universitas Indonesia, Indonesia
[2]Bioprocess Engineering Lab., Department of Chemical Engineering, Universitas Indonesia, Indonesia

Abstract
Effective control of methanol–water distillation is essential in dimethyl ether (DME) production due to strong nonlinearities and multivariable interactions. This study presents a comparative evaluation of fuzzy self-tuning proportional–integral (FSTPI) controllers with different initialization strategies in a 4×4 multivariable distillation system. Three variants—working-space (FSTPI-WS), working-range (FSTPI-WR), and PI-initialized FSTPI (FSTPI-PI Tuned)—are benchmarked against conventional PI controllers using a validated dynamic model implemented in MATLAB/Simulink with a C-based S-function for real-time adaptation. Controller performance is evaluated under ±5% setpoint changes and realistic disturbances in feed temperature and flow rate using integral absolute error (IAE), integral squared error (ISE), and interaction analysis. The results demonstrate that initialization strategy critically determines adaptive control performance. The FSTPI-PI Tuned consistently achieves the best performance, reducing IAE and ISE by more than 98% in the most interactive loop (condenser liquid level). For temperature-induced disturbances, IAE and ISE reductions exceed 98% and 99%, respectively. These findings indicate that fuzzy self-tuning is most effective when applied as an adaptive refinement layer atop a well-tuned PI controller, rather than as a standalone compensation mechanism, thereby providing a practical and computationally efficient solution for multivariable distillation control.

Keywords:
Dimethyl ether (DME);
Disturbance rejection;
Fuzzy self-tuning PI controller;
Initialization strategy;
Methanol-water distillation;
Multivariable control;

Article History:
Received: October 21, 2026
Revised: March 23, 2026
Accepted: April 27, 2026
Published: October 2, 2026

Corresponding Author:
Abdul Wahid
Process Systems Engineering Lab., Department of Chemical Engineering, Universitas Indonesia, Depok 16424, Indonesia
Email: wahid@che.ui.ac.id

INTRODUCTION

Dimethyl ether (DME) has emerged as a strategic clean fuel and chemical intermediate due to its high cetane number, soot-free combustion, and compatibility with existing liquefied petroleum gas (LPG) infrastructure. Recent reviews and industrial perspectives highlight DME's growing relevance in the global energy transition, both as a bridge fuel and as a flexible energy carrier synthesized from natural gas, biomass, or CO_2-derived syngas [1]–[3]. Industrial DME production is predominantly realized via the indirect route, in which methanol synthesized from syngas is subsequently dehydrated over acidic catalysts [4], [5]. Despite significant progress in catalyst development and process intensification, the dehydration reaction inevitably generates water, making downstream methanol–water purification a critical unit operation to ensure catalyst stability, product purity, and overall energy efficiency [6]–[8].

Methanol–water purification is typically performed using high-purity distillation columns that operate under stringent product specifications. From a control perspective, such columns exhibit pronounced nonlinear dynamics, strong multivariable interactions, transport delays, and high sensitivity to feed temperature and flow disturbances [9][10]. Integrated and intensified methanol distillation configurations further increase the dynamic coupling between energy and mass-transfer phenomena, thereby exacerbating control complexity [11]. As a result, methanol–water separation in DME production represents a highly interactive multivariable (4×4 MIMO) control problem, where inadequate regulatory control can directly lead to excessive energy consumption, off-spec products, and accelerated catalyst deactivation.

A wide range of methodologies has been proposed in the chemical process systems engineering literature to address operational complexity and reliability. Risk-oriented frameworks, including data-driven Failure Mode and Effects Analysis (FMEA) and fuzzy AHP–FMEA approaches, have been widely applied for offline hazard identification and static decision support [12][13]. These methods are effective for identifying critical failure scenarios and prioritizing risk mitigation actions at the design or planning stage. However, their inherently static nature limits their ability to evaluate real-time control performance, particularly with respect to loop-resolved dynamics, transient responses, and the propagation of interactions under disturbances. As a result, they do not capture the time-domain control behavior required to assess multivariable control performance in industrial systems. Therefore, this study focuses on dynamic, loop-resolved performance evaluation under realistic disturbances, complementing existing risk-based approaches and bridging the gap between static risk assessment and real-time control analysis.

In addition to risk-based approaches, advanced design and optimization methodologies, such as Bayesian optimization, surrogate-based optimization, and modern Design of Experiments (DOE) extensions, have been successfully applied to DME and methanol-based processes to explore operating windows and parametric sensitivities [14][15]. However, these approaches primarily rely on steady-state or quasi-steady assumptions. They are therefore unsuitable for capturing transient MIMO dynamics, nonlinear loop interactions, and disturbance-driven control trade-offs that dominate industrial distillation column operation [9][10].

Recent advances in data-driven statistical modeling and machine learning techniques, including principal component analysis (PCA), partial least squares (PLS), and soft sensors, have significantly improved process monitoring, fault detection, and inference in chemical separation systems [16]. Parallel developments in kinetic and mechanistic modeling of DME synthesis and separation processes further enhance process understanding and design [17]. Nevertheless, these approaches operate primarily at the supervisory or diagnostic level and do not replace the need for robust regulatory control strategies capable of maintaining product specifications under dynamic disturbances.

At the regulatory control layer, decentralized proportional–integral (PI) controllers remain the dominant industrial solution due to their simplicity, transparency, and ease of implementation. However, numerous studies on high-purity methanol distillation report that fixed-parameter PI controllers often exhibit degraded performance in strongly interacting and nonlinear systems, particularly under varying operating conditions and disturbances [9][18]. Multivariable model predictive control (MPC) has demonstrated superior decoupling and disturbance rejection capabilities in methanol–water separation, including validated 4×4 MIMO applications directly relevant to DME purification [19]–[21]. Despite these advantages, MPC performance depends strongly on model accuracy and fixed tuning structures, which may limit adaptability under nonlinear behavior and unmeasured disturbances.

Adaptive control strategies based on fuzzy logic, particularly fuzzy self-tuning PI (FSTPI) controllers, have therefore attracted renewed interest as a compromise between simplicity and adaptability. By adjusting PI gains online as functions of control error and its rate of change, FSTPI controllers offer a computationally efficient means of enhancing robustness. Over the past decade, self-tuning fuzzy PI and PID controllers have been successfully applied in power electronics, electric drives, power quality control, robotics, and aerospace systems, demonstrating improved disturbance rejection and adaptability compared to fixed-gain PI controllers [22]–[26]. In the context of separation processes, fuzzy-based control has also been reported to improve distillation column performance [27]. However, most existing studies focus on single-input single-output (SISO) systems, low-order MIMO configurations, or a single fuzzy rule-base structure, and typically provide qualitative or aggregate performance assessments.

Consequently, despite the extensive use of FSTPI in the literature, a clear research gap remains in the systematic, quantitative, and loop-resolved benchmarking of multiple fuzzy self-tuning PI initialization strategies in highly interactive, industrially relevant distillation systems. In particular, the role of controller initialization—such as WS [26], WR, and PI-derived variants—in shaping loop-specific performance, interaction behavior, and trade-offs between servo and regulatory objectives has not been explicitly investigated for validated 4×4 methanol–water distillation models representative of DME production. The baseline model and PI control structure are adopted from Wahid and Rikimata (2021) [19], which provides a validated multivariable distillation model and serves as a reference for evaluating controller improvements.

To address this gap, an appropriate control framework must balance adaptability, computational efficiency, and practical implementability in industrial environments. FSTPI control is therefore selected in this study because it provides a practical compromise between industrial simplicity and adaptive capability. Unlike model predictive control, which relies on accurate process models and higher computational effort, FSTPI can be implemented as an extension of conventional PI controllers while improving robustness under nonlinear and time-varying conditions. This makes it particularly suitable for highly interactive distillation systems where model uncertainty and process coupling are significant.

Rather than proposing a new fuzzy inference mechanism, mathematical formulation, or stability proof, this study introduces an initialization-centric and loop-resolved evaluation framework for FSTPI control in a highly interactive industrial distillation system. Through systematic and quantitative benchmarking under identical servo and regulatory scenarios, it is demonstrated that the effectiveness of FSTPI is decisively governed by the quality of its baseline PI controller. Optimized PI-based initialization enables fuzzy adaptation to operate as a refinement mechanism rather than a compensatory one, resulting in substantial performance improvements in dominant and highly interactive loops.

This study makes three main contributions. First, it provides a quantitative and loop-resolved comparison of multiple FSTPI initialization strategies in a realistic 4×4 distillation system. Second, it introduces a unified evaluation framework that integrates servo and regulatory performance with interaction analysis. Third, it demonstrates that controller initialization fundamentally determines the effectiveness of fuzzy adaptation in multivariable systems.

METHOD

This study employs a structured experimental workflow to evaluate the performance of multiple FSTPI controllers and conventional PI controllers on a validated 4×4 methanol–water distillation model. The methodology consists of five major stages as shown in Figure 1.

4×4 Multivariable Distillation Model

The simulation model used in this study is based on the methanol–water purification system reported by Wahid and Rikimata (2021), represented as a multivariable transfer function model:

$$\mathbf{Y}(s) = \mathbf{G}(s)\mathbf{U}(s) + \mathbf{G_d}(s)\mathbf{D}(s) \qquad (1)$$

where $\mathbf{Y}(s) \in \mathbb{R}^{4\times1}$ is the vector of controlled variables (CVs), $\mathbf{U}(s) \in \mathbb{R}^{4\times1}$ is the vector of manipulated variables (MVs), and $\mathbf{D}(s) \in \mathbb{R}^{2\times1}$ represents disturbances.

The CV vector is defined as:

$$\mathbf{Y}(s) = \begin{bmatrix} T_{\text{cond}} \\ T_{\text{cooler}} \\ L_{\text{cond}} \\ L_{\text{column}} \end{bmatrix}$$

Moreover, the MV vector is:

$$\mathbf{U}(s) = \begin{bmatrix} Q_{\text{cond}} \\ Q_{\text{cooler}} \\ F_D \\ F_B \end{bmatrix}$$

The disturbance vector is:

$$\mathbf{D}(s) = \begin{bmatrix} F_F \\ T_F \end{bmatrix}$$

The process transfer function matrix $\mathbf{G}(s) \in \mathbb{R}^{4\times4}$ and disturbance matrix $\mathbf{G_d}(s) \in \mathbb{R}^{4\times2}$ are modeled using first-order plus dead-time (FOPDT) dynamics:

$$G_{ij}(s) = \frac{K_{ij}e^{-\theta_{ij}s}}{\tau_{ij}s+1} \qquad (2)$$

where K_{ij}, τ_{ij}, and θ_{ij} represent process gain, time constant, and dead time, respectively. The complete numerical matrices are adopted from Wahid and Rikimata (2021) and are provided in Table 1 and Table 2 for clarity and reproducibility.

Implementation of Conventional PI Controllers

Conventional PI controllers are first implemented as a baseline for comparison. The PI control law is:

$$u(t) = K_c\, e(t) + K_i \int_0^t e(\tau)\, d\tau \qquad (3)$$

with:

$$e(t) = r(t) - y(t) \qquad (4)$$

The initial PI parameters reported in Wahid and Rikimata (2021) were adopted as the nominal values. These parameters represent practical controller settings used in previous distillation control studies.

To generate an improved PI benchmark, MATLAB PID Tuner was used to obtain:

$$(K_c, K_i)_{\text{MPIDT}} \tag{5}$$

Tuning criteria were based on:

- response speed,
- overshoot minimization, and
- acceptable degree of controller aggressiveness.

The tuned PI controller serves both as a performance benchmark and as a basis for constructing one of the fuzzy rule structures (FSTPI-MPIDT).

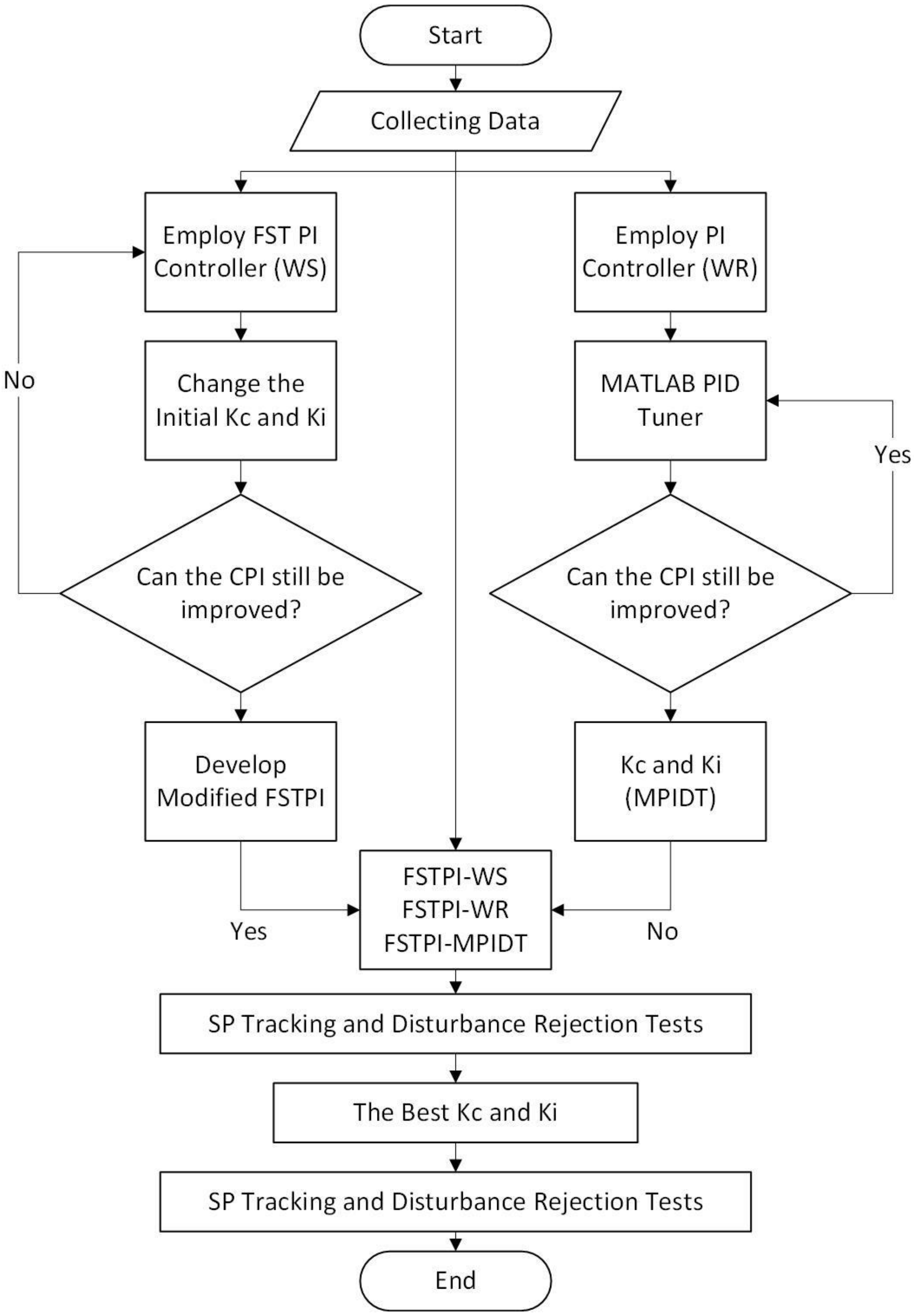

Figure 1. Research steps

Table 1. Transfer function parameters of the 4×4 distillation model

MV	CV	K_{ij}	t_{ij}	q_{ij}
Q_{cond}	T_{cond}	-0.20000	0.150	0.680
Q_{cooler}	T_{cond}	-0.01200	1.120	7.400
F_D	T_{cond}	0.58400	0.030	0.050
F_B	T_{cond}	0.00060	1.320	0.570
Q_{cond}	T_{cooler}	0.00800	2.400	6.290
Q_{cooler}	T_{cooler}	-0.50200	0.330	0.010
F_D	T_{cooler}	-0.00400	0.750	0.460
F_B	T_{cooler}	-0.000200	0.270	1.001
Q_{cond}	L_{cond}	-0.00100	0.750	1.170
Q_{cooler}	L_{cond}	0.03000	0.660	0.050
F_D	L_{cond}	-0.0003	0.750	0.350
F_B	L_{cond}	0.00007	0.270	0.150
Q_{cond}	L_{column}	-0.07320	0.150	0.350
Q_{cooler}	L_{column}	-0.04900	1.320	1.210
F_D	L_{column}	-0.00700	1.635	0.420
F_B	L_{column}	-0.32000	0.760	0.020

Table 2. Disturbance transfer function parameters

D	CV	K_{ij}	t_{ij}	q_{ij}
F_F	T_{cond}	0.0001	1.000	1.150
F_F	T_{cooler}	-0.0065	3.625	8.323
F_F	L_{cond}	0.00003	1.376	1.723
F_F	L_{column}	0.0016	3.000	7.950
T_F	T_{cond}	0.1066	1.633	2.478
T_F	T_{cooler}	0.0902	1.500	2.475
T_F	L_{cond}	0.0148	1.325	1.945
T_F	L_{column}	-0.0275	3.000	9.450

Development and Implementation of FSTPI Controllers

The FSTPI controller extends the conventional PI controller by adapting the proportional and integral gains online based on the control error and its rate of change. The error signals are defined as:

$$e(t) = r(t) - y(t), \dot{e}(t) = \frac{de(t)}{dt} \tag{6}$$

A Mamdani-type fuzzy inference system is employed, in which both error and error rate are mapped to linguistic variables. In this study, seven linguistic terms are used: Negative Big (NB), Negative Medium (NM), Negative Small (NS), Zero (ZO), Positive Small (PS), Positive Medium (PM), and Positive Big (PB). Triangular membership functions are adopted for all input variables due to their simplicity and computational efficiency.

The scaling and normalization parameters, defined as $\varepsilon_1 = 0.008$, $\varepsilon_2 = 0.003$, $\varepsilon_3 = 0.0005$, and $\lambda = 30000$, determine the sensitivity of the fuzzy inference system and influence the gain adaptation behavior.

The fuzzy rule base computes incremental adjustments to the controller gains as:

$$\Delta K_c = f_1(e, \dot{e}), \Delta K_i = f_2(e, \dot{e}) \tag{7}$$

where the rule base encodes expert knowledge, such as increasing proportional gain for large errors and adjusting integral gain to eliminate steady-state deviations.

The controller gains are updated online according to:

$$K_c(t) = K_{c0} + \Delta K_c(t),\ K_i(t) = K_{i0} + \Delta K_i(t) \tag{8}$$

where $K_{c0}$and K_{i0}represent the initial gains. In this study, three initialization strategies are evaluated:

- FSTPI-WS (working-space initialization)
- FSTPI-WR (working-range initialization)
- FSTPI-PI Tuned (PI-based initialization)

C-Based S-Function Implementation

To ensure real-time gain adaptation, FSTPI controllers were coded in C using a Simulink S-function structure. The S-function includes:

- mdlInitializeSizes(): defining states, inputs, and outputs
- mdlInitializeSampleTimes(): setting the sampling period
- mdlOutputs(): computing fuzzy inference and generating control action
- mdlUpdate(): updating internal states and parameter adjustments
- mdlTerminate(): clearing resources

This ensures deterministic execution and compatibility with real-time simulation.

Development of Modified FSTPI

If the Control Performance Index (CPI) indicates that the controller can still be improved, the rule base, membership functions, or initial gains are modified. This stage produces three candidate controllers:

1. FSTPI-WS [26]
2. FSTPI-WR: Wahid–Rudi PI controller tuning method is formulated as follows:

$$K_c = \frac{0.0672\tau + 1.774}{K_p},\ K_i = \frac{K_c}{1.027\tau + 10.777} \tag{9}$$

where $K_p$and τrepresent the process gain and dead time, respectively, which are parameters of the first-order plus dead-time (FOPDT) model.

3. FSTPI-MPIDT

Each controller represents a different strategy for handling nonlinearities and dynamic interactions in the 4×4 column presented in Table 3.

Table 3. Comparison of Kc and Ki Values from WR and MATLAB PID Tuning

Parameter	CV1	CV2	CV3	CV4
PI-WR Kc	0.667	4.905	0.007	13.503
PI-WR Ki	0.333	42.409	2.160	2.378
PI-Tuned Kc	1.074	6.414	0.050	40.942
PI-Tuned Ki	2.532	2.364	48.532	0.301
Unadjusted RT	1543	0.209	3.071	0.769
Unadjusted TB	0.600	0.600	0.600	0.600
Suitable RT	3.875	0.209	412.1	0.116
Suitable TB	0.774	0.882	0.594	0.720

Setpoint and Disturbance Rejection Experiments

Each controlled variable (CV) shown in Figure 2 is subjected to setpoint variations of ±5%, defined relative to its baseline operating value:

$$\Delta r = \pm 0.05\, r_0 \tag{10}$$

where r_0 denotes the baseline setpoint, these variations are selected to represent moderate yet realistic industrial perturbations that are sufficient to excite process dynamics while remaining within normal operating limits.

Due to inherent multivariable coupling, a disturbance applied to one loop propagates to other loops. This allows evaluation of cross-interaction handling, robustness to internal coupling, and the trade-off between controller aggressiveness and stability.

In addition to setpoint changes, realistic operating disturbances in feed flow rate (F_F) and feed temperature (T_F) are introduced with ±5% variations relative to their baseline values. These disturbances reflect common industrial fluctuations and are used to assess disturbance-attenuation capability, resilience to nonlinearities, and the propagation of interactions across CVs.

The control performance is evaluated using integral error metrics. In this study, the CPI is defined in terms of the Integral of Absolute Error (IAE) and Integral of Squared Error (ISE), which quantify overall tracking accuracy and penalize large deviations, respectively:

$$\text{IAE} = \int_0^{t_f} |\, e(t)\, |\; dt \tag{11}$$

$$\text{ISE} = \int_0^{t_f} e^2\,(t)\, dt \tag{12}$$

Lower CPI values indicate better control performance.

Controller Selection and Verification

The best-performing controller for each CV is selected based on:

- minimum IAE and ISE,
- stable dynamic response,
- robustness to disturbances,
- minimal interaction-induced oscillations.

Selected controllers are then subjected to integrated setpoint and disturbance rejection tests to verify their consistency and suitability for multivariable distillation applications.

RESULTS AND DISCUSSION

PI Controller SP Change Test

The optimized PI controller demonstrates a clear improvement in dynamic performance compared with the default WR tuning across most controlled variables during setpoint change tests. Visual inspection of the closed-loop responses (Figure 3) indicates faster rise times, significantly improved damping, and shorter settling behavior for the tuned controller, particularly for the dominant condenser-related loops.

Quantitatively (Table 4 and 5), substantial performance gains are observed on the primary (diagonal) loops, especially for CV1 and CV3. For CV1 (condenser temperature), the tuned controller reduces the Integral of Absolute Error (IAE) by 99.87% and the Integral of Squared Error (ISE) by 88.30%, indicating a near-elimination of steady-state deviation and oscillatory behavior. The most pronounced improvement occurs on CV3 (condenser liquid level), where primary-loop IAE and ISE decrease by 79.23% and 89.49%, respectively, reflecting a transition from poorly damped oscillations under default tuning to a near-critically damped response under optimized parameters.

In contrast, CV2 and CV4 exhibit more limited or mixed improvements on their primary loops. In particular, the primary-loop IAE of CV2 increases slightly under the tuned parameters, suggesting that aggressive tuning does not uniformly enhance performance across all loops in this highly interactive system.

Beyond primary-loop behavior, tuning's impact on loop interactions (off-diagonal elements) offers important insights. Setpoint changes applied to CV3 yield the most substantial reduction in cross-coupling effects, with reductions in interaction IAE ranging from approximately 78% to nearly 100% for the other controlled variables. Similarly, interaction ISE values decrease consistently by around 89%, including a large absolute reduction in the CV3→CV1 interaction, where ISE drops from approximately 68,900 to 7,450. These results indicate that the optimized tuning not only improves CV3's own response but also significantly attenuates its disturbance propagation to other loops.

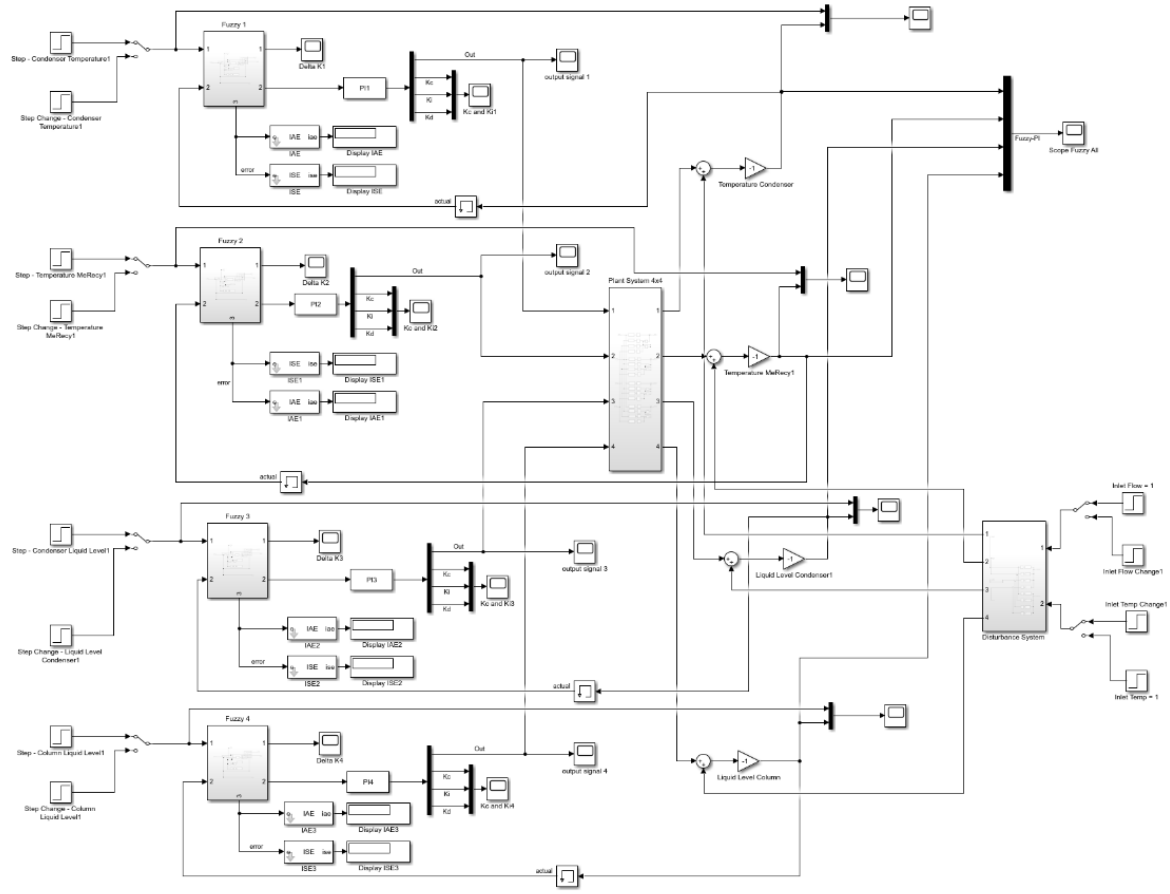

Figure 2. Full layout of the multi-loop PI controller simulation in Simulink

Conversely, setpoint changes on CV2 produce the opposite trend. Interaction effects increase markedly, most notably on CV3, where the interaction IAE rises from a negligible value to several units, representing an increase of several orders of magnitude. This behavior indicates that, for CV2, the tuned controller sacrifices decoupling performance in favor of faster local response, amplifying cross-loop interactions.

Overall, the optimized PI parameters deliver substantial improvements over the default WR tuning for the dominant condenser-related loops, particularly CV1 and CV3, and significantly reduce interaction effects when CV3 is perturbed. However, the results also highlight an inherent trade-off in multivariable PI control: aggressive tuning that enhances speed and damping for selected loops can exacerbate interactions for others. These findings strongly support the use of systematic, application-specific tuning rather than default heuristics, and suggest that further performance enhancement—especially for highly interactive loops such as CV2—may require explicit decoupling strategies or advanced multivariable control approaches, such as centralized MPC.

PI Controller Disturbance Test

Figure 4 and Table 6–7 summarize the closed-loop responses of CV1–CV4 under three disturbance scenarios: inlet temperature disturbance (IT), inlet flow rate disturbance (IF), and combined temperature–flow disturbance (ITF). Compared with the default WR parameters, the PI controller tuned with the MATLAB PID Tuner demonstrates markedly superior disturbance rejection to temperature-driven upsets, which are the most severe disturbances in this process.

For temperature-related disturbances (IT and ITF), the largest improvements are observed on CV3 (condenser liquid level). Under IT disturbances, CV3 IAE is reduced from 1,370 to 291 (≈78.8%), while ISE decreases from 1,890 to 204 (≈89.2%). Similar improvements are obtained under ITF disturbances, with IAE decreasing from 1,330 to 284 (≈78.7%) and ISE from 1,800 to 194 (≈89.2%). These results indicate substantially improved damping and faster recovery for the dominant inventory-controlled loop.

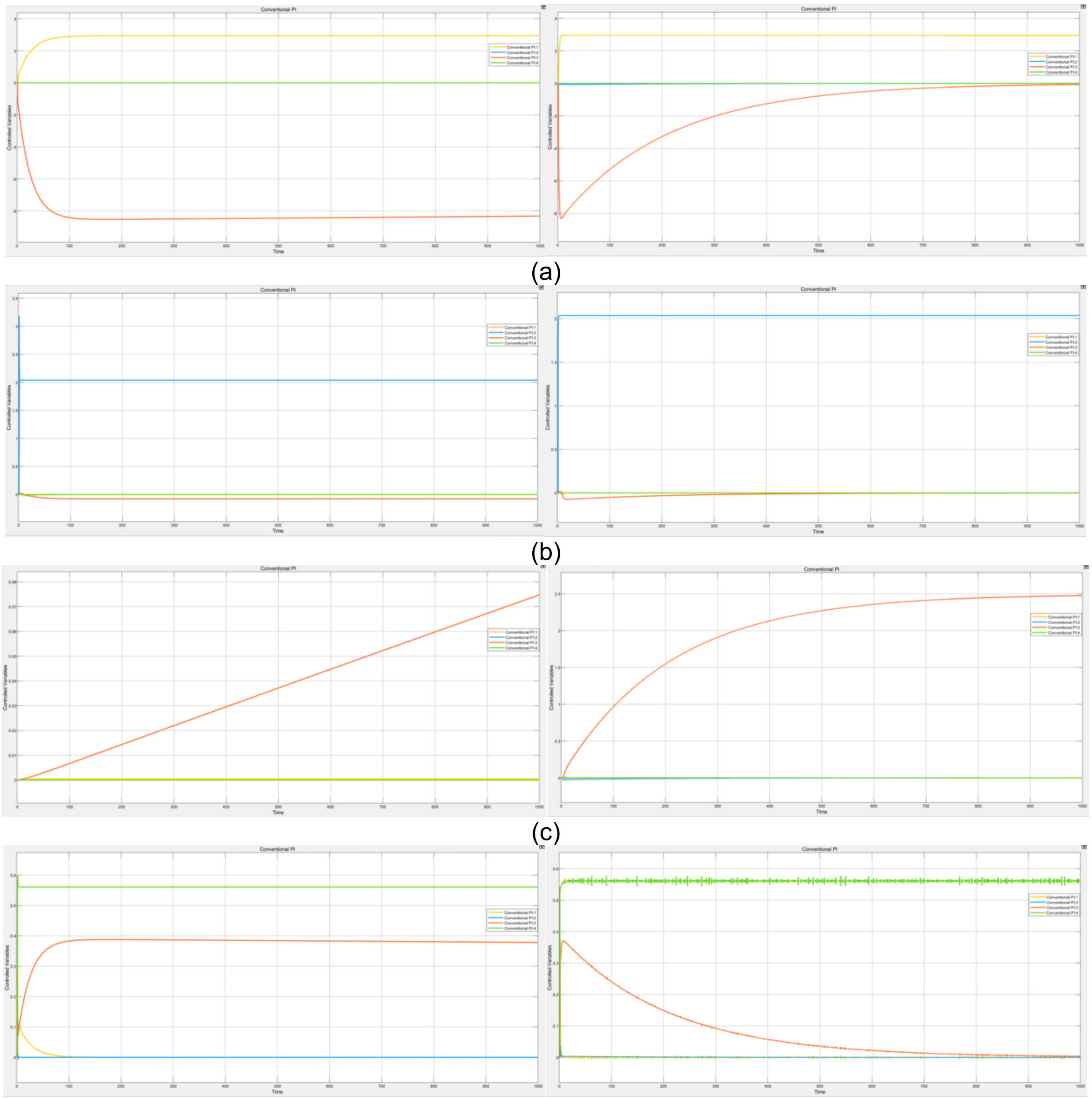

(a) (b) (c) (d)

Figure 3. PI-WR and PI-Tuner SP change test: (a) CV1, (b) CV2, (c) CV3, and (d) CV4

Table 4. Comparison of IAE values from PI controller SP change test

CV	PI – WR				PI - Tuned			
	CV1	CV2	CV3	CV4	CV1	CV2	CV3	CV4
CV1	67.00	0.74	0.42	2.96	0.09	0.09	1.16	0.68
CV2	0.04	0.36	0.01	0	0.42	0.42	4.87	0.78
CV3	8,260	75.20	2,460	376	16.3	16.3	511	79.7
CV4	0	0	0	0.11	0.01	0.01	0.33	1.05

Table 5. Comparison of ISE values from PI controller SP change test

CV	PI - WR				PI - Tuned			
	CV1	CV2	CV3	CV4	CV1	CV2	CV3	CV4
CV1	88.9	0.01	0	0.19	10.4	0	0	0.04
CV2	0	0.31	0	0	0.67	0.24	0.06	0
CV3	68,900	5.77	6,050	143	7,450	0.64	636	15.4
CV4	0	0	0	0.03	0	0	0	0.02

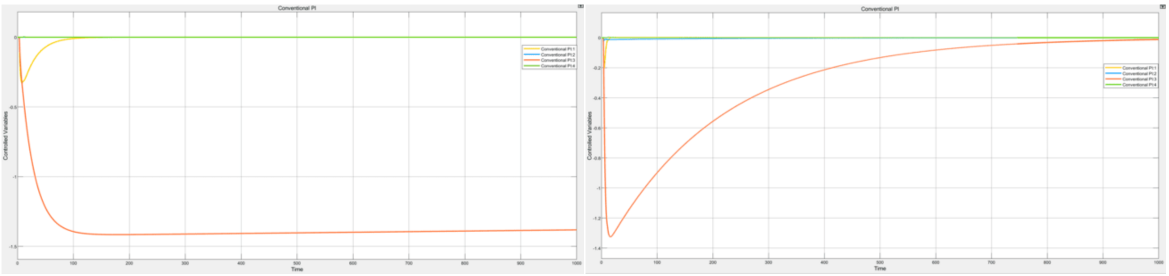

(a)

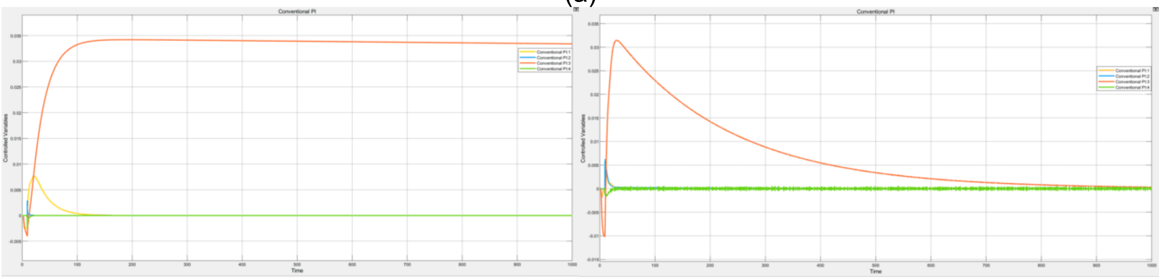

(b)

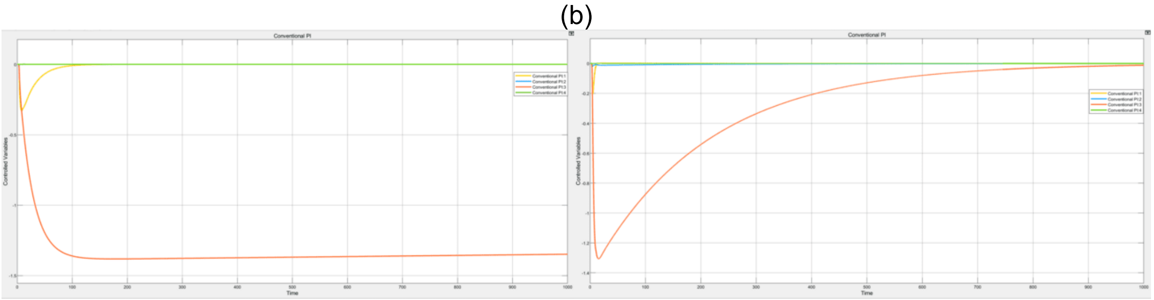

(c)

Figure 4. PI Controller (WR Parameters) and (MATLAB PID Tuner) Disturbance Test: (a) temperature inlet, (b) flow rate inlet, (c) temperature and flow rate inlet

Table 6. Comparison of IAE cause of temperature IT, IF, ITF disturbance test

CV	PI -WR			PI - Tuned		
	IT	IF	ITF	IT	IF	ITF
CV1	10.7	0.32	10.4	1.48	0.07	1.42
CV2	0.01	0	0.01	2.82	0.1	2.73
CV3	1,370	32.6	1,330	291	7.15	284
CV4	0.01	0.01	0.01	0.67	0.09	0.44

Table 7. Comparison of ISE cause of temperature IT, IF, ITF disturbance test

CV	PI -WR			PI - Tuned		
	IT	IF	ITF	IT	IF	ITF
CV1	2.03	0.00147	1.96	0.108	0.0000759	0.108
CV2	0.0000175	0.00000139	0.0000188	0.0194	0.000122	0.018
CV3	1,890.00	1.09	1,800.00	204	0.12	194
CV4	0.0000243	0.00000538	0.0000188	0.00053	0.0000288	0.000229

Significant gains are also achieved on CV1 (condenser temperature). For IT and ITF disturbances, CV1 ISE is reduced by approximately 94.5–94.8%, confirming enhanced thermal regulation and reduced peak deviations under tuned PI control. Visual inspection of the disturbance responses (Figure 4a and 4c) further supports these quantitative findings, showing smoother trajectories and faster stabilization for the tuned controller.

In contrast, flow rate disturbances (IF) produce relatively small baseline errors under the default WR tuning. Nevertheless, the tuned PI controller still achieves meaningful reductions on CV3, with IAE and ISE decreasing by approximately 78% and 89%, respectively. However, these improvements are accompanied by degraded performance on secondary loops, particularly CV2 and CV4, where both IAE and ISE increase under tuned parameters.

Overall, the disturbance test results demonstrate that the tuned PI controller substantially enhances regulatory performance under temperature-induced disturbances, particularly in the primary-affected loops CV1 and CV3. At the same time, increased sensitivity to flow disturbances and amplified cross-variable responses on CV2 and CV4 highlight a robustness trade-off inherent to aggressive single-loop tuning in multivariable systems.

Trade-off Between Servo and Regulatory Performance

The combined analysis of setpoint change and disturbance rejection tests reveals a consistent performance pattern. Under setpoint changes, the tuned PI controller delivers substantial improvements in speed, damping, and integral error metrics for the dominant condenser-related loops, particularly CV1 and CV3. These gains demonstrate the effectiveness of systematic, application-specific tuning compared with default heuristic parameters.

The disturbance tests further confirm that these improvements extend to regulatory performance when temperature-related disturbances dominate. The tuned controller achieves 78–95% reductions in IAE and ISE on CV1 and CV3 for IT and ITF disturbances, indicating robust rejection of the most critical process upsets.

However, both tests consistently reveal a trade-off. While aggressive tuning enhances performance on dominant loops, it increases cross-variable sensitivity and degrades performance on secondary loops, most notably CV2 and, to a lesser extent, CV4. This behavior reflects the inherent limitation of decentralized PI control in highly interactive systems, where improvements in servo and regulatory performance for selected loops can amplify interactions elsewhere.

These findings emphasize that performance gains observed in setpoint tracking do not automatically guarantee uniformly improved disturbance rejection across all variables. Instead, they highlight the need to balance speed, damping, and robustness when tuning PI controllers in multivariable processes.

FSTPI Control Performance Test

Figure 5 and Tables 8 – 10 present a comparative evaluation of three fuzzy self-tuning PI (FSTPI) controller variants—FSTPI-WS, FSTPI-WR, and FSTPI-PI Tuned—under setpoint changes applied to the four controlled variables (CV1–CV4). The results clearly demonstrate that controller initialization plays a decisive role in determining both transient performance and multivariable interaction behavior.

Under FSTPI-WS initialization, the closed-loop responses exhibit relatively slow convergence, noticeable overshoot, and persistent oscillations, particularly in the interacting loops. This behavior is most evident when the condenser liquid level (CV3) is excited, where large baseline errors are observed (IAE = 1450 and ISE = 2450). Significant interaction effects propagate to CV1 and CV2, indicating limited damping capability and weak suppression of cross-loop coupling.

The FSTPI-WR variant provides a clear improvement over FSTPI-WS. Primary-loop IAE and ISE values are consistently reduced, and the closed-loop responses show improved damping and shorter settling behavior. Nevertheless, residual low-frequency oscillations remain visible, especially in CV3 responses, suggesting that while the Wahid–Rikimata initialization enhances stability margins, it does not fully resolve the strong process interactions.

The FSTPI-PI Tuned variant achieves the best overall performance. Across the dominant primary loops (CV1–CV3), this controller achieves substantial reductions in integral error metrics compared with FSTPI-WS. Primary-loop IAE is reduced by 78.4% for CV1, 76.7% for CV2, and 98.2% for CV3, while corresponding ISE reductions reach up to 98.7% for CV3. Visual inspection of Figure 5 confirms that these quantitative gains translate into minimal overshoot, near-monotonic convergence, and markedly faster settling behavior.

In addition to primary-loop improvements, FSTPI-PI Tuned demonstrates superior suppression of interaction effects when highly interactive variables are excited. For setpoint changes applied to CV3, average reductions of approximately 98–99% in both IAE and ISE are achieved across secondary loops, indicating effective attenuation of disturbance propagation in the most challenging dynamic scenario. These results confirm that initializing the fuzzy self-tuning mechanism with optimized PI parameters significantly enhances both local loop performance and the handling of multivariable interactions.

However, the results also reveal important trade-offs. For CV4, which exhibits relatively weak baseline interaction under FSTPI-WS, the aggressive adaptation of FSTPI-PI Tuned increases the primary-loop error (IAE) by approximately 65%.

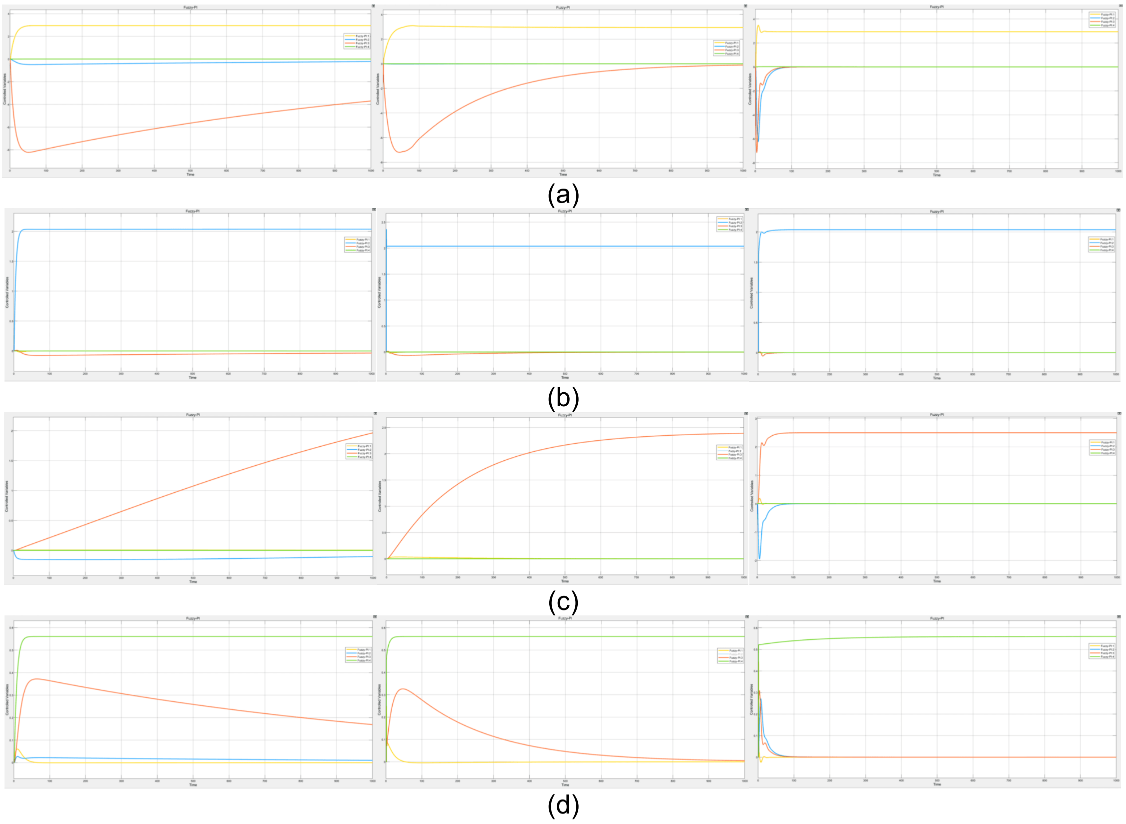

Figure 5. FSTPI control (Initial WS Parameters), (WR Parameters), (Tuned Parameters) CV1 Change Test

Table 8. Comparison of IAE and ISE from FSTPI-WS control on SP change test

CV	IAE				ISE			
	CV1	CV2	CV3	CV4	CV1	CV2	CV3	CV4
CV1	41.2	0.493	5.79	2.06	51.8	0.0043	0.0342	0.0617
CV2	340	11.7	138	15.8	123	9.43	19.2	0.265
CV3	5,720	52.4	1,450	259	34,600	2.94	2,450	71.4
CV4	1.42	0.0183	0.577	4.18	0.0021	2E-06	0.0003	1.2

Table 9. Comparison of IAE and ISE from FSTPI-WR control on SP change test

CV	IAE				ISE			
	CV1	CV2	CV3	CV4	CV1	CV2	CV3	CV4
CV1	69.6	0.663	8.99	2.88	59.6	0.0063	0.182	0.113
CV2	5.95	0.324	1.68	0.276	0.0763	0.265	0.0067	0.0002
CV3	1,960	18.2	617	88.9	8,240	0.703	765	16.9
CV4	0.436	0.0051	0.126	0.757	0.0004	2E-07	4E-05	0.0646

Table 10. Comparison of IAE and ISE from FSTPI-PI Tuned control on SP change test

CV	IAE				ISE			
	CV1	CV2	CV3	CV4	CV1	CV2	CV3	CV4
CV1	8.91	0.075	1.46	0.378	11.8	0.0005	0.178	0.0448
CV2	108	2.73	31.5	4.98	363	0.626	32.6	0.685
CV3	88.1	0.949	25.7	3.99	325	0.0268	32.6	0.611
CV4	3.48	0.0403	1.04	6.91	0.0374	5E-06	0.0034	0.14

Mixed interaction behavior is also observed for CV2-initiated setpoint changes, highlighting the difficulty of achieving uniform performance across all loops using decentralized fuzzy self-tuning alone.

FSTPI control Disturbance Test

Figure 6 and Tables 11 – 12 present the disturbance rejection performance of the three fuzzy self-tuning PI (FSTPI) controller variants—FSTPI-WS, FSTPI-WR, and FSTPI-PI Tuned—under inlet temperature (IT), inlet flow rate (IF), and combined temperature–flow (ITF) disturbances. The results clearly indicate that temperature-related disturbances dominate the process dynamics and constitute the most severe operating scenarios, particularly for the condenser liquid level (CV3).

Under IT and ITF disturbances, the FSTPI-PI Tuned controller delivers the most pronounced performance improvements on the primary affected loops. For CV3, which exhibits the largest baseline sensitivity, IAE is reduced from 948 (FSTPI-WS) to 14.6 under IT disturbance, corresponding to a reduction of approximately 98.5%, while ISE decreases from 955 to 7.36 (≈99.2%). Similar levels of improvement are observed under ITF disturbances. These results demonstrate a substantial enhancement in damping and recovery speed for the dominant inventory-controlled loop.

Significant gains are also achieved on CV1 (condenser temperature). Under IT disturbance, the Tuned variant reduces IAE by approximately 85% and ISE by nearly 89% relative to the WS initialization, indicating markedly improved thermal regulation and attenuation of temperature-induced transients. While the FSTPI-WR controller provides partial improvement over FSTPI-WS, it is consistently outperformed by the Tuned variant for temperature-driven disturbances, often by more than one order of magnitude on CV3.

In contrast, pure flow disturbances (IF) produce substantially smaller baseline errors across all controller variants, particularly on CV1 and CV3. Even in this less demanding scenario, the FSTPI-PI Tuned controller achieves near-complete suppression of residual errors on the primary loops, with CV3 IAE and ISE reduced to 0.132 and 0.004, respectively. Extremely low residual errors are also observed on CV1 and CV2 under IF conditions, confirming the strong adaptability of the Tuned variant. The FSTPI-WR controller maintains stable and balanced performance under flow disturbances, although it is generally outperformed by the Tuned controller on the most affected loops.

Despite its superior regulatory performance on CV1 and CV3, the FSTPI-PI Tuned controller exhibits notable trade-offs on secondary loops. Under IT disturbances, CV2 experiences a substantial increase in IAE relative to the WR variant, and CV4 exhibits elevated error levels in several temperature-sensitive cases. This behavior reflects the inherent trade-off of aggressive adaptive tuning: optimizing for rapid stabilization of dominant, highly interactive loops can increase sensitivity in less critical or weakly coupled loops. By comparison, the FSTPI-WR variant offers more uniform cross-loop robustness, albeit at the expense of slower recovery and higher residual errors on the primary loops.

This behavior requires further analysis in terms of multivariable interaction dynamics. The strong coupling between thermal and inventory loops in the distillation system can explain the increased interaction effects observed in CV2 under temperature disturbances. Energy dynamics directly influence CV2 (cooler temperature) and are tightly coupled with both the condenser temperature (CV1) and condenser liquid level (CV3). When temperature disturbances are introduced, they propagate rapidly through the thermal network, affecting multiple loops simultaneously.

Under these conditions, aggressive adaptive actions in dominant loops—particularly CV1 and CV3—can amplify interaction effects in CV2. The control efforts aimed at stabilizing temperature and inventory introduce variations in heat duty and internal flows, which are subsequently reflected in the cooler temperature loop. As a result, CV2 experiences increased oscillations and higher integral error values despite improvements in the primary loops.

Furthermore, compared to the inventory-controlled CV3, CV2 exhibits faster thermal dynamics and higher sensitivity to upstream disturbances, making it more susceptible to interaction-induced fluctuations. This highlights a fundamental limitation of decentralized adaptive control: performance improvements in dominant loops can come at the expense of increased interaction in secondary loops.

Overall, the disturbance test results confirm that the FSTPI-PI Tuned controller provides the most effective rejection of severe temperature-induced disturbances, achieving reductions exceeding 98% in IAE and 99% in ISE on the critical condenser liquid level loop. The findings further underscore the decisive role of initialization strategy in fuzzy self-tuning control. Optimized PI-based initialization enables the fuzzy mechanism to focus on fine-scale adaptation rather than compensating for fundamental loop deficiencies, resulting in markedly superior regulatory performance.

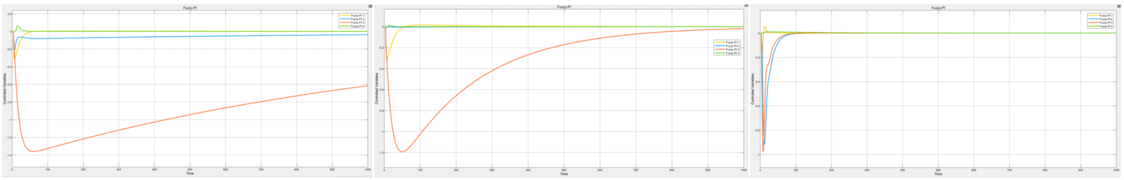

(a)

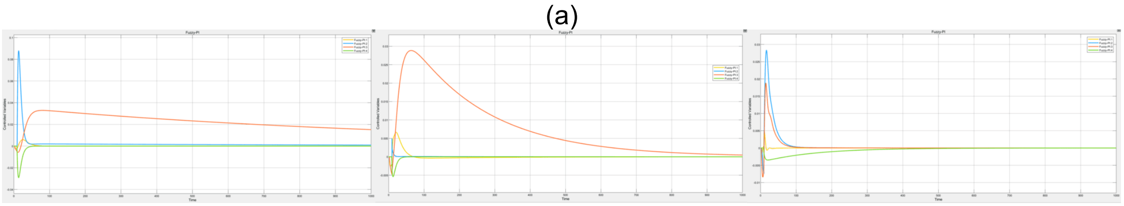

(b)

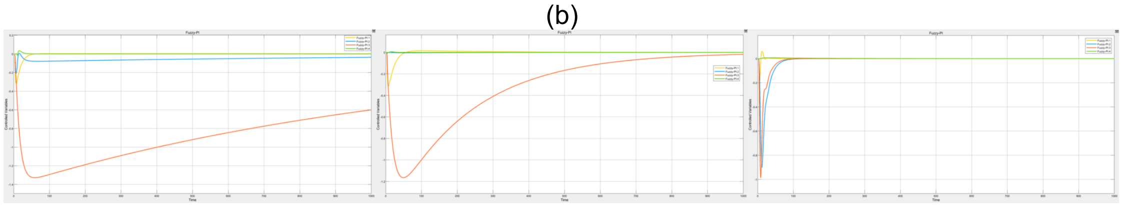

(c)

Figure 6. FSTPI control (Initial WS Parameters), (WR Parameters), (Tuned Parameters) Inlet Temperature Disturbance Test

Table 11. Comparison of IAE cause of temperature IT, IF, ITF disturbance test

CV	FSTPI-WS			FSTPI-WR			FSTPI-PI Tuned		
	IT	IF	ITF	IT	IF	ITF	IT	IF	ITF
CV1	7.47	0.23	0.23	10.4	0.0304	0.299	1.11	9E-04	0.03
CV2	58.2	2.39	2.39	1.01	0.675	0.0344	18.3	2E-05	0.675
CV3	948	22.7	22.7	324	0.45	7.89	14.6	0.132	0.45
CV4	1.06	0.394	0.394	0.22	0.562	0.0712	1.75	3E-04	0.562

Table 12. Comparison of ISE cause of temperature IT, IF, ITF disturbance test

CV	FSTPI-WS			FSTPI-WR			FSTPI-PI Tuned		
	IT	IF	ITF	IT	IF	ITF	IT	IF	ITF
CV1	1.05	0.0007	7E-04	1.26	0.0009	0.0009	0.116	8E-05	8E-05
CV2	3.68	0.0637	0.064	0.002	2E-05	2E-05	9.29	0.01	0.01
CV3	955	0.5540	0.554	225	0.132	0.132	7.36	0.004	0.004
CV4	0.03	0.0075	0.008	0.001	0.0003	0.0003	0.0099	0.001	0.001

For applications requiring more uniform robustness across diverse disturbance types, the results suggest that further enhancements—such as interaction-aware fuzzy rules or explicit decoupling strategies—may be necessary. This behavior is consistent with classical multivariable control theory, where strong loop interactions can lead to unavoidable performance trade-offs under decentralized control structures.

From PI Control to FSTPI under Servo and Regulatory Scenarios

The combined evaluation of conventional PI and fuzzy self-tuning PI (FSTPI) controllers across both setpoint change (servo) and disturbance rejection (regulatory) scenarios provides a comprehensive understanding of the evolution of control performance in this multivariable thermal separation process. The results consistently show that control effectiveness is governed not only by tuning aggressiveness but, more fundamentally, by the quality of the baseline control structure on which fuzzy adaptation mechanisms operate.

The optimized PI controller establishes a critical baseline. In setpoint change tests, systematic PI tuning significantly improves the transient response and damping of the dominant condenser-related loops, particularly CV1 (condenser temperature) and CV3 (condenser liquid level). However, these improvements are accompanied by increased cross-loop interactions for certain excitations, highlighting the inherent limitations of decentralized PI control in strongly coupled systems.

While model-based multivariable control strategies such as model predictive control (MPC) could potentially provide improved decoupling and coordinated control action, the observed improvements in the FSTPI-PI Tuned controller suggest that substantial performance gains can already be achieved through improved baseline shaping, without requiring full multivariable optimization or explicit model-based coordination.

Under disturbance conditions, the tuned PI controller achieves strong rejection of temperature-induced disturbances but exhibits reduced robustness for flow disturbances and secondary loops, confirming that single-loop tuning alone cannot fully address multivariable interaction effects.

The setpoint change results further highlight the role of adaptive mechanisms. Rule-based initializations (FSTPI-WS and FSTPI-WR) provide adaptability beyond static PI control but remain constrained by the quality of initial loop shaping. FSTPI-WS exhibits slow convergence and oscillatory behavior due to insufficient damping, while FSTPI-WR improves stability but retains residual oscillations. In contrast, the FSTPI-PI Tuned variant consistently delivers superior performance, particularly for CV3, with IAE and ISE reductions exceeding 98%. This improvement is primarily attributed to the well-tuned PI baseline, which provides a well-damped response and enables the fuzzy mechanism to serve as a refinement layer rather than a compensatory tool.

For CV3, an inventory-controlled variable dominated by accumulation dynamics and strong thermal coupling, PI-based initialization significantly reduces oscillations and steady-state deviations, allowing the adaptive mechanism to operate within a narrower error range. Consequently, gain adaptation becomes more stable and effective, while reduced disturbance propagation from temperature-controlled loops (e.g., CV1) further enhances performance.

The disturbance rejection results reinforce this interpretation. Temperature-related disturbances (IT and ITF), driven by energy–mass coupling, represent the most challenging scenarios. Under these conditions, the FSTPI-PI Tuned controller achieves the most effective attenuation, reducing IAE and ISE for CV3 by more than 98% and 99%, respectively, while also improving performance in CV1. Although the FSTPI-WR variant provides balanced performance—particularly under flow disturbances—it is consistently outperformed under severe thermal upsets.

Overall, the results reveal a consistent hierarchy: static PI control provides essential baseline stability but is limited by interaction effects; rule-based FSTPI improves adaptability yet remains constrained by initialization quality; and FSTPI-PI Tuned integrates optimized linear control with adaptive refinement to achieve superior performance in dominant and highly interactive loops. The observed degradation in secondary loops (e.g., CV2 and CV4) highlights an inherent trade-off of decentralized adaptive control, where aggressive stabilization of dominant variables may increase sensitivity in weaker loops.

These findings confirm that initialization strategy is a decisive factor in fuzzy self-tuning PI control. Optimized PI-based initialization enables effective refinement rather than compensation, resulting in superior servo and regulatory performance. Further improvements toward balanced multivariable robustness may require interaction-aware fuzzy rules, explicit decoupling strategies, or integration with centralized control frameworks.

CONCLUSION

The results demonstrate that while optimized PI control significantly improves baseline performance, its effectiveness is inherently constrained by multivariable interaction effects in decentralized control architectures.

FSTPI controllers enhance adaptability beyond static PI control; however, their performance is strongly governed by the quality of the baseline PI parameters. Among the evaluated strategies, the FSTPI-PI Tuned consistently delivers the best performance, achieving reductions exceeding 98% in integral error metrics for the dominant condenser liquid level loop under both setpoint changes and temperature-induced disturbances, while effectively suppressing oscillatory behavior.

Despite these improvements, performance degradation observed in secondary loops highlights an inherent trade-off between aggressive stabilization of dominant variables and uniform robustness across all control loops. These findings confirm that fuzzy self-tuning is most effective when applied as an adaptive refinement layer built upon a well-tuned PI controller, rather than as a standalone replacement for sound linear control design.

From a practical perspective, the proposed FSTPI-PI Tuned strategy offers strong potential for industrial implementation. It can be deployed as an extension of existing PI-based control architectures with minimal structural modification, making it suitable for retrofitting in distributed control systems (DCS) while maintaining low computational requirements for real-time operation.

Future work should explore hybrid approaches incorporating interaction-aware fuzzy rules, explicit decoupling strategies, and integration with centralized multivariable control frameworks such as model predictive control (MPC). In addition, systematic benchmarking against alternative advanced control strategies—including IMC-based PI, adaptive PID, and learning-based controllers (e.g., ANFIS or reinforcement learning)—would enable a more comprehensive evaluation of performance and implementation trade-offs across model-based, rule-based, and learning-based control paradigms in strongly coupled processes.

Overall, the findings indicate that substantial performance improvements can be achieved through enhanced controller initialization alone, without increasing structural or computational complexity, offering a practical and scalable pathway for industrial multivariable control applications.

ACKNOWLEDGMENT

We express our gratitude to Universitas Indonesia, which has funded this research through the Hibah Seed Funding Professor Scheme No. NKB-3443/UN2.F4.D/DPPM.00.00/2024.

REFERENCES

[1] C. Peinado, A. Urtiaga, J. J. Aguayo, and J. Bilbao, "Review and perspective: Next generation DME synthesis technologies for the energy transition," *Chemical Engineering Journal*, vol. 479, Art. no. 147494, 2024, doi: 10.1016/j.cej.2023.147494

[2] A. Singh, S. Bhattacharya, and P. Basu, "Syngas generation for methanol synthesis: Oxy-steam gasification route using agro-residue as fuel," *Biomass Conversion and Biorefinery*, vol. 12, no. 5, pp. 1–15, 2022, doi: 10.1007/s13399-021-02128-y

[3] M. Sarić, J. Marković, and K. V. Gernaey, "Sorption-enhanced DME synthesis provides high flexibility: Evidence from modeling industrial use cases," *Industrial Chemistry & Materials*, 2025, doi: 10.1039/D4IM000XX

[4] N. Delgado Otalvaro, J. M. Grau, and J. Pérez-Ramírez, "Kinetics of the direct DME synthesis from CO_2-rich syngas," *RSC Advances*, vol. 11, no. 41, pp. 24556–24569, 2021, doi: 10.1039/D1RA03452A

[5] G. Bonura, F. Arena, and F. Frusteri, "Promoting direct CO_2 conversion to DME over zeolite-based hybrid catalysts," *Petroleum Chemistry*, vol. 60, no. 5, pp. 508–515, 2020, doi: 10.1134/S096554412005003X

[6] T. J. Deka, S. N. Upadhyay, and A. K. Chatterjee, "Methanol fuel production, utilization, and techno-economy: A review," *Environmental Chemistry Letters*, vol. 20, no. 4, pp. 2823–2859, 2022, doi: 10.1007/s10311-022-01485-y

[7] M. M. Emtir and A. A. Elbabour, "Energy integration and reactive distillation for dimethyl ether synthesis," *Chemical Engineering Transactions*, vol. 88, pp. 1141–1146, 2021, doi: 10.3303/CET2188190

[8] S. Wild, M. Studt, and J. Pérez-Ramírez, "Direct DME synthesis on CZZ/H-FER from variable CO_2/CO syngas feeds," *RSC Advances*, vol. 11, no. 5, pp. 2556–2568, 2021, doi: 10.1039/D0RA09754C

[9] S. B. Halager, I. A. Udugama, and K. V. Gernaey, "Regulatory and advanced control structures for high-purity methanol distillation," *Chemical Engineering Research and Design*, vol. 165, pp. 1–12, 2021, doi: 10.1016/j.cherd.2020.10.015

[10] I. A. Udugama, S. B. Halager, and K. V. Gernaey, "Modeling and control of integrated high-purity methanol distillation," *Chemical Engineering Research and Design*, vol. 175, pp. 1–12, 2021, doi: 10.1016/j.cherd.2021.08.024

[11] B. Ervural and H. I. Ayaz, "A fully data-driven FMEA framework for risk assessment on manufacturing processes using a hybrid approach," *Engineering Failure Analysis*, vol. 152, Art. no. 107525, 2023, doi: 10.1016/j.engfailanal.2023.107525

[12] I. Perić, K. Klarić, A. Pirc Barčić, K. Vukman, T. Sedlar, and P. Grošelj, "Optimizing risk management in wood-based manufacturing: A fuzzy AHP-FMEA framework approach," *BioResources*, vol. 20, no. 2, pp. 2979–3001, 2025, doi: 10.15376/biores.20.2.2979-3001

[13] N. Delgado Otalvaro, J. M. Grau, and J. Pérez-Ramírez, "Robust design of a DME production process using Bayesian optimization," *Industrial & Engineering Chemistry Research*, vol. 62, no. 32, pp. 12645–12658, 2023, doi: 10.1021/acs.iecr.3c01567

[14] L. F. Zubeir, R. L. Smith, and M. J. Martín, "Stripping-enhanced distillation for renewable CO_2-to-DME purification," *Separations*, vol. 10, no. 7, Art. no. 403, 2023, doi: 10.3390/separations10070403

[15] A. Melo, M. M. Câmara, and J. C. Pinto, "Data-driven process monitoring and fault diagnosis: A comprehensive survey," *Processes*, vol. 12, no. 2, Art. no. 251, 2024, doi: 10.3390/pr12020251

[16] M. Ghavipour, A. Abedi, and J. Pérez-Ramírez, "Kinetic modeling of direct DME synthesis over hybrid catalysts," *Catalysts*,

vol. 14, no. 1, Art. no. 61, 2024, doi: 10.3390/catal14010061

[17] S. B. Halager, I. A. Udugama, and K. V. Gernaey, “Advanced control of high-recovery methanol distillation,” *Chemical Engineering Research and Design*, vol. 175, pp. 1–12, 2021, doi: 10.1016/j.cherd.2021.08.024

[18] A. Wahid and Z. H. Brillianto, “Multivariable model predictive control (4×4) of methanol–water separation in DME production,” *AIP Conference Proceedings*, vol. 2255, Art. no. 030055, 2020, doi: 10.1063/5.0013764

[19] A. Wahid and M. Rikimata, “Methanol–water purification control using multi-loop PI controllers,” *ChemEngineering*, vol. 5, no. 4, Art. no. 70, 2021, doi: 10.3390/chemengineering5040070

[20] S. B. Halager, I. A. Udugama, and K. V. Gernaey, "Modeling and control of integrated methanol distillation configurations," *Chemical Engineering Research and Design*, vol. 175, pp. 1–12, 2021, doi: 10.1016/j.cherd.2021.08.024

[21] A. Kaysal, M. Yilmaz, and H. Çelik, “DC–DC converter based self-tuning fuzzy PI controller,” *Journal of the Faculty of Engineering and Architecture of Gazi University*, vol. 38, no. 1, pp. 483–495, 2023.

[22] Y. Cui and D. Gan, “Fuzzy PI control in voltage-mode PWM rectifiers,” *Proceedings of SPIE*, vol. 12790, Art. no. 1279048, 2023, doi: 10.1117/12.2689896

[23] R. Li, Z. Wang, and Y. Chen, “Fuzzy control strategy for CHB-STATCOM under grid faults,” in *Proceedings of the IEEE IPEMC–ECCE Asia*, 2024, doi: 10.1109/IPEMC.2024.XXXX

[24] A. Fekik, A. Boukhelifa, and M. Benyettou, “Modeling and simulation of quadcopter using self-tuning fuzzy PI control,” in *Mobile Robot: Motion Control and Path Planning*, Springer, 2023, pp. 231–251, doi: 10.1007/978-3-031-XXXX-X_10

[25] M. Tajjudin, N. A. Rahman, and S. Abdullah, “Design and evaluation of self-tuning fuzzy PID control,” *International Journal of Emerging Technology and Advanced Engineering*, vol. 12, no. 8, pp. 196–203, 2022.

[26] A. Wahid, S. Anandita, M. F. Fadlian, and A. H. Mendrofa, “Improvement of linear distillation column control performance using fuzzy self-tuning PI controller,” *AIP Conference Proceedings*, vol. 2255, Art. no. 030061, 2020, doi: 10.1063/5.0014060

[27] S. Banivaheb, S. Pitter, and M. Grilc, “Recent progress in direct dimethyl ether synthesis and potential of bifunctional catalysts,” *Chemie Ingenieur Technik*, vol. 93, no. 10, pp. 1505–1515, 2021, doi: 10.1002/cite.202100078